

## CALCULATION OF DAY AND NIGHT EMITTANCE VALUES

## FOR DEATH VALLEY, CALIFORNIA

Anne B. Kahle

Jet Propulsion Laboratory  
 California Institute of Technology  
 Pasadena, CA 91109

In July 1983, the TIMS was flown over Death Valley, California on both a midday and predawn flight within a two-day period. The availability of calibrated digital data permitted the calculation of day and night surface temperature and surface spectral emittance.

Image processing of the data included panorama correction and calibration to radiance using the on-board black bodies and the measured spectral response of each channel (Palluconi and Meeks, 1985). Scene-dependent isolated-point noise due to bit drops, was located by its relatively discontinuous values and replaced by the average of the surrounding data values. Bad lines were repaired using values interpolated from adjacent lines. Coherent noise due to microphonics was not removed in these data as it had been in earlier data sets (Kahle, 1983) because it was not judged to be too severe. Both day and night decorrelation-stretched color composite images were created for this Death Valley data set with bands 1, 3, and 5 displayed in blue, green, and red, respectively. As noted in our earlier papers, with this particular band-color display, quartz-rich rocks appear red, carbonates blue-green, and volcanics and shales blue to purple in these images. Comparison of the day-night pair showed that the hues, corresponding to emittance, are similar in the various rock units, while the most striking differences between images are in the intensity of various units, explainable on the basis of day-night temperature effects.

In order to separate the spectral and temperature information contained in these TIMS data, a method is used that was developed by Kahle et al. (1980). It is assumed that the emittance of the ground at every point is equal to 0.93 in the wavelength region of channel six (11.3-11.6  $\mu\text{m}$ ). Then Planck's Law

$$L_{\lambda} = \epsilon_{\lambda} W_B(\lambda, T) = \frac{\epsilon_{\lambda} C_1}{\lambda^5 [\exp(C_2/\lambda T) - 1]}$$

where:  $L_{\lambda}$  = measured radiance  
 $W_B$  = blackbody radiance  
 $\lambda$  = wavelength  
 $T$  = temperature  
 $C_1$  = first radiation constant  
 $C_2$  = second radiation constant and  
 $\epsilon_{\lambda}$  = emittance,

is solved numerically for ground temperature for each pixel in channel 6. Using these temperature values, Planck's Law is then solved in each of the other channels for emittance  $\epsilon_{\lambda}$ .

Both day and night data sets were processed by the above method. There are significant differences to be seen in the day and night temperature images which, as indicated above, were derived from channel 6. In the day image, shaded or north-facing slopes are cooler (darker) than the sun-facing slopes. This illumination-aspect effect disappears in the night image. The very high Panamint Mountains are cold at night due to radiative cooling. Two other areas exhibit striking day-night temperature differences. Middle Basin, in the bottom of the valley floor, has standing water that keeps the area relatively cool (dark) in the day image and relatively warm (bright) in the night image. Conversely, Furnace Creek Fan is very hot in the day image and very cold in the night image. This fan, composed of very low thermal inertia material, bakes dry and becomes very hot in the daytime. At night, water entering the valley at Furnace Creek apparently makes its way to the surface where significant evaporative cooling takes place. A similar effect, of much more limited extent, can be seen at the bottom of the fans coming out of the Panamint Mountains. The ability to detect this effect could be very useful in hydrologic studies.

The emittance images, which were created for channels 1 through 5 for both the day and night data, are shown in Figure 1 with high emittance areas bright. In addition, channels 1, 3, and 5 of the emittance were displayed in blue, green, and red using the decorrelation stretch, for both the day and night data sets. The similarity of the day and night images demonstrates that the procedure for removing the temperature and displaying only emittance is at least qualitatively correct. The emittance images of channel 5 for both day and night (Figure 1) appear quite noisy. This is an artifact introduced by assuming that all emittance values in channel 6 are equal to a constant. Because the emittance in channel 5 is correlated to that in channel 6, it also is being forced towards a constant value -- leaving small dynamic range in the image.

Spectral differences among rock units are consistent from day to night. In Figure 1 the very darkest (low emittance) units in channel 1 are the Eureka and Stirling Quartzite. This is attributed to the strong quartz bands ascribed to the silicon-oxygen stretching vibration (Hunt and Salisbury, 1974). The relatively low emittance of the quartzite becomes less pronounced with increasing wavelength. Alluvial fans which contain abundant quartzite clasts in an argillaceous matrix, such as the prominent Tucki Wash and Trail Canyon Fan, are also quite dark, as are their source areas. Spectrally flat carbonates and their derived fans are bright (relatively high emittance) in all channels. The most noticeable changes with wavelength are in the volcanic units including the small andesite outcrop located in the Tucki Wash. These volcanics have a fairly high relative emittance in channel 1 which decreases with increasing wavelength through channel 4, the location of the reststrahlen band of these silicates. These observations are all predictable from laboratory observations (Lyon, 1965).

TIMS is unique in allowing collection of both spectral emittance and thermal information in digital format with the same airborne scanner. For the first time it has been possible to produce day and night emittance images of the same area, coregistered. These data add to an understanding of the physical basis for the discrimination of differences in surface materials afforded by TIMS.

The research described in this paper was carried out by the Jet Propulsion Laboratory, California Institute of Technology, under contract with the National Aeronautics and Space Administration.

#### REFERENCES

- Hunt, G.R., and Salisbury, J. W., 1974, Mid-infrared spectral behavior of igneous rocks: AFCRL-TR-74-0625.
- Kahle, A. B., 1983, The new airborne Thermal Infrared Multispectral Scanner (TIMS): IEEE, Proc. International Geoscience and Remote Sensing Symposium (IGARSS '83) II, 7.1-7.6.
- Kahle, A.B., Madura, D. P., and Soha, J. M., 1980, Middle infrared multispectral aircraft scanner data: analysis for geological applications: Appl. Optics, 19, 2279-2290.
- Lyon, R.J.P., 1965, Analysis of rocks by spectral infrared emission (8 to 25 microns): Econ. Geol., 60, 715-736.
- Palluconi, F. D., and Meeks, G. R., 1985, Thermal Infrared Multispectral Scanner (TIMS): an investigator's guide to TIMS data: Jet Propulsion Lab. Pub. 85-32.

ORIGINAL PAGE IS  
OF POOR QUALITY

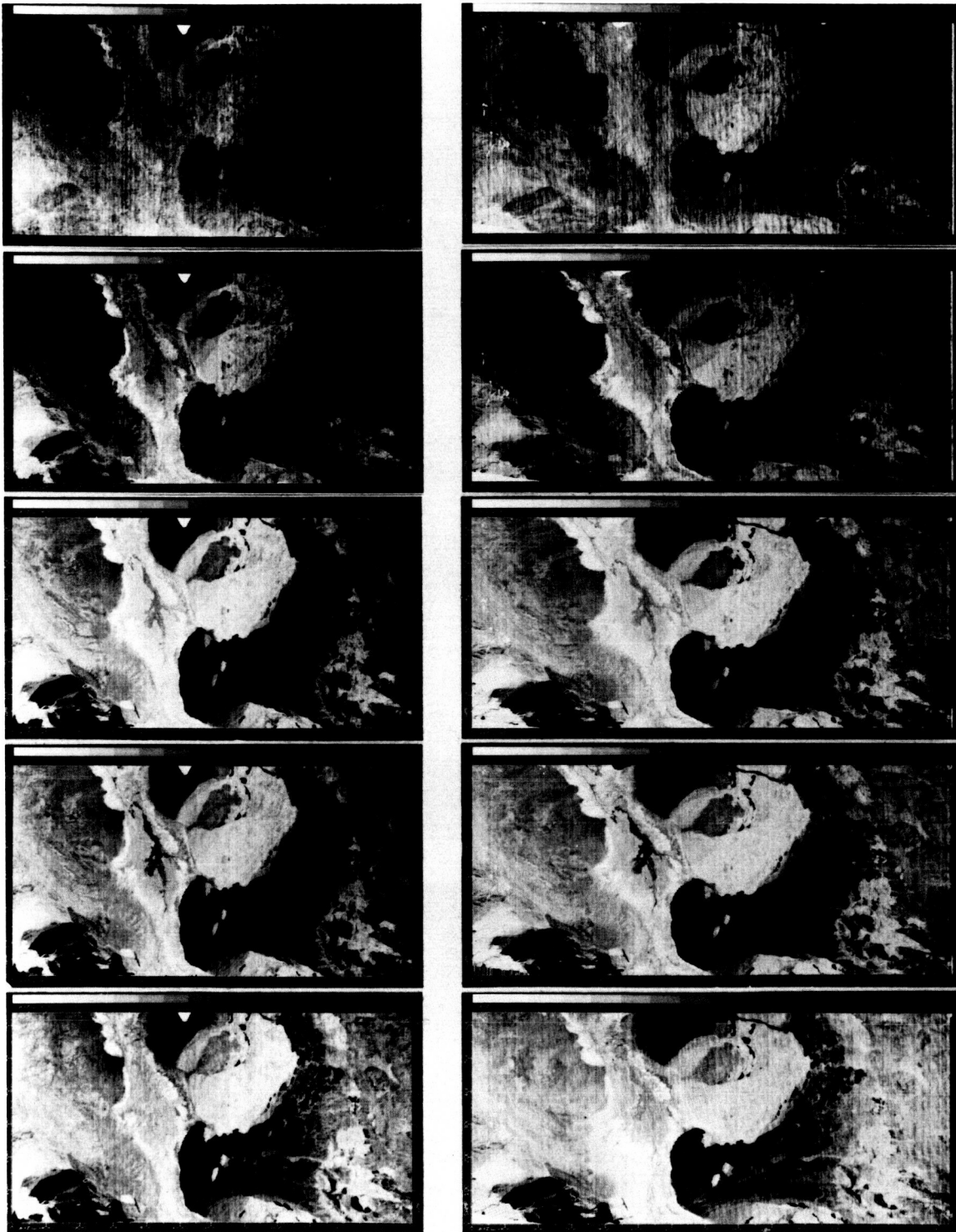


Fig. 1. Emittance images. Top row is emittance derived from the day flight; channels 1-5 from left to right. Bottom row is the emittance derived from the night data.